

LA-UR- 09-04519

Approved for public release;
distribution is unlimited.

Title:

Computation of Multi-Material Interactions Using Material Point Method

Author(s):

Duan Z. Zhang- T-3
Xia Ma- T-3
Paul Giguere- T-3

Intended for:

International Conference on Particle Based Methods

Nov. 25-27, 2009, Barcelona, Spain



Los Alamos National Laboratory, an affirmative action/equal opportunity employer, is operated by the Los Alamos National Security, LLC for the National Nuclear Security Administration of the U.S. Department of Energy under contract DE-AC52-06NA25396. By acceptance of this article, the publisher recognizes that the U.S. Government retains a nonexclusive, royalty-free license to publish or reproduce the published form of this contribution, or to allow others to do so, for U.S. Government purposes. Los Alamos National Laboratory requests that the publisher identify this article as work performed under the auspices of the U.S. Department of Energy. Los Alamos National Laboratory strongly supports academic freedom and a researcher's right to publish; as an institution, however, the Laboratory does not endorse the viewpoint of a publication or guarantee its technical correctness.

Computation of Multi-Material Interactions Using Material Point Method

LA-UR 09-01018

D. Z. Zhang, X. Ma and P. T. Giguere

Fluid Dynamics and Solid Mechanics Group,
Theoretical Division,
Los Alamos National Laboratory,
T-3, B216,
Los Alamos, NM 87545, USA
dzhang@lanl.gov

Abstract

Calculations of fluid flows are often based on Eulerian description, while calculations of solid deformations are often based on Lagrangian description of the material. When the Eulerian descriptions are used to problems of solid deformations, the state variables, such as stress and damage, need to be advected, causing significant numerical diffusion error. When Lagrangian methods are used to problems involving large solid deformations or fluid flows, mesh distortion and entanglement are significant sources of error, and often lead to failure of the calculation. There are significant difficulties for either method when applied to problems involving large deformation of solids. To address these difficulties, particle-in-cell (PIC) method is introduced in the 1960s. In the method Eulerian meshes stay fixed and the Lagrangian particles move through the Eulerian meshes during the material deformation. Since its introduction, many improvements to the method have been made. The work of Sulsky et al. (1995, *Comput. Phys. Commun.* v.87, pp. 236) provides a mathematical foundation for an improved version, material point method (MPM), of the PIC method.

The unique advantages of the MPM method have led to many attempts of applying the method to problems involving interaction of different materials, such as fluid-structure interactions. These problems are multiphase flow or multimaterial deformation problems. In these problems pressures, material densities and volume fractions are determined by satisfying the continuity constraint. However, due to the difference in the approximations between the material point method and the Eulerian method, erroneous results for pressure will be obtained if the same scheme used in Eulerian methods for multiphase flows is used to calculate the pressure. To resolve this issue, we introduce a numerical scheme that satisfies the continuity requirement to higher order of accuracy in the sense of weak solutions for the continuity equations. Numerical examples are given to demonstrate the new scheme.

COMPUTATION OF MULTI-MATERIAL INTERACTIONS USING MATERIAL POINT METHOD

DUAN Z. ZHANG, XIA MA AND PAUL T. GIGUERE

Fluid Dynamics and Solid Mechanics Group
Theoretical Division
Los Alamos National Laboratory
Los Alamos, NM 87545, USA
e-mail: dzhang@lanl.gov

Key words: Material Point Method, Multiphase Flow, Fluid-Structure Interaction.

Summary. This paper describes the application of the material point method to compute interactions of materials undergoing large deformation on the basis of an averaged equation model. The main focus is on the numerical schemes of the material point method needed to compute material interactions.

1 INTRODUCTION

Calculations of fluid flows are often based on an Eulerian description, while calculations of solid deformations are often based on a Lagrangian description of the material. When Eulerian descriptions are used on problems of solid deformations, the state variables, such as stress and damage, need to be advected, causing significant numerical diffusion error. When Lagrangian methods are used on problems involving large solid deformations or fluid flows, mesh distortion and entanglement are significant sources of error, and often lead to failure of the calculation. There are significant difficulties for either method when applied to problems involving large deformation of solids. To address these difficulties, the particle-in-cell (PIC) method was introduced in the 1960s. In the PIC method the Eulerian mesh stays fixed and the Lagrangian particles move through the Eulerian mesh during the material deformation. Since its introduction, many improvements to the method have been made. The work [1] of Sulsky et al. provides a mathematical foundation for an improved version, the material point method (MPM), of the PIC method.

The unique advantages of MPM have led to many attempts to apply the method to problems involving interactions of different materials, such as fluid-structure interactions, projectile-target interactions, and impact of an object on a structure. Such applications of MPM encountered unique issues absent from a calculation for a single material. These issues include satisfying continuity conditions in mixed cells which contain two or more materials, and calculation of material acceleration in these cells. Due to the difference in the numerical approximations between the material point method and the Eulerian method, erroneous results and instabilities will be obtained if the commonly used schemes in Eulerian methods for multiphase flows are used. The purpose of the present paper is to describe schemes proven effective in resolving these issues in the application of MPM to problems involving interactions of materials.

2 AVERAGED EQUATIONS FOR MATERIAL INTERACTIONS

The starting point of our work is the system of averaged equations for multi-material interactions. The MPM is used to solve the continuum equations for the materials involved. The material points are used as Lagrangian points to trace motions in the continua. Unlike particles in a discrete element method (DEM) or in a molecular dynamic (MD) simulation, where particles interact directly with each other through prescribed force laws, in MPM, material points, sometime also called particles, do not interact directly with each other. The effects of their interactions are considered on the mesh nodes according to the constitutive relation of the materials. The motion of a material is described by a system of partial differential equations with the volume fraction, velocity and stress of the material defined everywhere in the computational domain.

This system of equations is obtained from the extension of averaged equations for disperse multiphase flows. In a disperse multiphase flow, there is only one continuous phase. All other phases are in the form of particles, droplets or bubbles with characteristic size much smaller than the problem domain. In problems involving multi-material interactions, such as fluid-structure interactions, often the interacting materials have sizes comparable to the size of the problem domain. For these problems the equations of motion for the materials have been derived [2]. For many practical cases the momentum equation for material i can be written as [2],

$$\frac{\partial \rho_i \mathbf{u}_i}{\partial t} + \nabla \cdot (\rho_i \mathbf{u}_i \mathbf{u}_i) = -\theta_i \nabla P + \nabla \cdot [\theta_i (\boldsymbol{\sigma}_i + P \mathbf{I})] + \mathbf{f}_i + \rho_i \mathbf{g}, \quad (1)$$

where \mathbf{u}_i is velocity of material i , ρ_i is the macroscopic density, θ_i is the volume fraction, P is the pressure in the system, $\boldsymbol{\sigma}_i$ is the stress in the material, \mathbf{f}_i is the interaction force acting on the material, and \mathbf{g} is the gravity acceleration. In this equation, the definition of force \mathbf{f}_i is related to the definition of the pressure P [2]. The model for force \mathbf{f}_i needs to consider many physical interactions, such as drag, lift, added mass force, and Basset force, in disperse multiphase flows. For many practical problems force \mathbf{f}_i can be simply modeled as a drag related to the relative motion of materials, and the pressure P is selected to be the pressure of the “softest” material or fluid in the problem. This momentum equation allows a material to have its own stress $\boldsymbol{\sigma}_i$ or pressure. This model of material interaction is called multi-pressure model. This is important for a problem involving interactions of many materials. For instance, in the study of breakup of a porous solid in air, the air pressure is always positive, while the solid material does not break without a tensile stress. Therefore it is important to allow for different stresses in different materials as in (1).

Momentum equation (1) is written in a form that is more convenient for solution using the MPM. To understand its physical meaning, we can write it as

$$\rho_i^0 \left(\frac{\partial \mathbf{u}_i}{\partial t} + \mathbf{u}_i \cdot \nabla \mathbf{u}_i \right) = \nabla \cdot \boldsymbol{\sigma}_i + (\boldsymbol{\sigma}_i + P \mathbf{I}) \cdot \frac{\nabla \theta_i}{\theta_i} + \frac{1}{\theta_i} \mathbf{f}_i + \rho_i^0 \mathbf{g}. \quad (2)$$

In this form, the first term on the right hand side represents acceleration due to stress divergences as in the momentum equations for a solid motion. The second term represents

surface traction on material interfaces. At the material interface $\nabla \theta_i$ is a vector with direction along the inward normal \mathbf{n} of the material. The magnitude of $\nabla \theta_i$ is of order $1/\Delta x$, where Δx is the mesh spacing. As the mesh is refined, the second term on right hand side of (2) becomes the traction force acting on the material interface.

This momentum equation together with the mass conservation equation for each material

$$\frac{\partial \rho_i}{\partial t} + \nabla \cdot (\rho_i \mathbf{u}_i) = 0, \quad (3)$$

and the continuity equation

$$\sum_{i=1}^M \theta_i = \sum_{i=1}^M \frac{\rho_i}{\rho_i^0(p_i)} = 1 \quad (4)$$

form a closed equation system when the constitutive models for stresses and the material interaction force are provided. Equation (4) is an additional requirement for multi-material interactions. For single material motion, the volume fraction for the material is always one; and (4) is satisfied automatically. For multi-material interactions or multiphase flows, this equation is used to determine the pressures in the materials.

3 MATERIAL POINT METHOD

The material point method is an advanced version of the PIC method developed by Harlow in 1960s. During the last half century, the PIC method has been applied to various problems, and has been improved along with the advances of computers and mathematical theory of numerical computation. Currently the MPM is based on the mathematical theory of weak solution to the governing equations [1]. This theory for MPM is extended here to solve the averaged equations for material interactions listed above. In this section, we only list the steps of MPM needed in a successful calculation of multi-material interactions. Readers interested in their derivations are referred to references [1] and [4]. These steps are either modified from or straightforward extension of the steps in the classical MPM method for computation of single material motions. The modified steps consider effects of material interactions which are absent in single material problems.

In a MPM, the domain is divided into cells similar to the finite volume method. As in the finite volume method, a node l is associated with a volume V_l . Differently from the finite volume method, we also put Lagrangian material points into the cells. Material point p of phase i is assigned a mass m_{ip} and a volume v_{ip} . Unless there is a phase change, the mass associated with a material point does not change during the calculation. Velocity of a material is calculated at nodes and at material points. Velocities defined on nodes and material points are related by shape function S_l defined on the mesh nodes. The finite volume mesh is Eulerian; it is fixed in the calculation. Material points are Lagrangian points; they follow motion of the material. They are used to track deformation history of the material. For this reason, in a material point method, the stress σ_{ip} of material i is calculated on the material points. The time advancement in a MPM is divided into a Lagrangian step and a material motion step, similar to the procedure in an arbitrary Lagrangian Eulerian (ALE) method. The Lagrangian step of the time advancement is based on momentum equation (1), and is discretized as [4]

$$m_{il} \frac{\mathbf{u}_{il}^L - \mathbf{u}_{il}^n}{\Delta t} = - \sum_{p=1} v_{ip} (\boldsymbol{\sigma}_{ip} + P\mathbf{I}) \cdot \nabla S_l(\mathbf{x}_{ip}) + (-\theta_i \nabla P + \mathbf{f}_i + \theta_i \rho_i \mathbf{g}) V_l , \quad (5)$$

where superscript L denotes the Lagrangian step and superscript n denotes the current time step, the summation is over the material points representing phase i in the domain, and m_{il} is the mass of material i in the control volume associated with on node l . The mass m_{il} on node l is calculated from the mass on the material point as

$$m_{il} = \sum_{p=1} m_{ip} S_l(\mathbf{x}_{ip}) , \quad (6)$$

where \mathbf{x}_{ip} is the position of material point p of phase i .

In (5) the Lagrangian velocities are calculated on the nodes. Then velocity on material point is updated by interpolating the Lagrangian velocity change to the material points as

$$\mathbf{u}_{ip}^{n+1} = \mathbf{u}_{ip}^n + \sum_{l=1}^N (\mathbf{u}_{il}^L - \mathbf{u}_{il}^n) S_l(\mathbf{x}_{ip}) , \quad (7)$$

where N is the number of nodes in the problem domain. The positions of the material points are updated with the velocity interpolated from the mesh node to the positions of the material points as

$$\mathbf{x}_{ip}^{n+1} = \mathbf{x}_{ip}^n + \sum_{l=1}^N 0.5 (\mathbf{u}_{il}^L + \mathbf{u}_{il}^n) S_l(\mathbf{x}_{ip}) \Delta t . \quad (8)$$

Using this updated velocity and positions of the material points, the velocity at a mesh node is updated as

$$\mathbf{u}_{il}^{n+1} = \sum_{p=1} m_{ip} \mathbf{u}_p^{n+1} S_l(\mathbf{x}_{ip}^{n+1}) / \sum_{p=1} m_{ip} S_l(\mathbf{x}_{ip}^{n+1}) . \quad (9)$$

The processes of updating the locations of the material points and then using the material point velocities to update the node velocities correspond to the advection process in an ALE calculation.

3.1 Calculation of strain rates

Steps described in (6) to (9) are the direct generalization from the MPM used in a calculation of a single material. Step (5) is also an extension of the method for a single material, but with additional terms. Although the pressure gradient term and the interaction force term appear only in multi-material interactions, they can be calculated straightforwardly as in an ALE method. The special issues related to material interactions in (5) concerns the mass m_{il} associated with node l . In a multi-material problem, the node may be near a material interface and the cells with node l may contain only one material point far away from the node. In this case, according to (6) the mass m_{il} associated with the node may be very small because of the small value of the shape function $S_l(\mathbf{x}_p)$. As a consequence, the acceleration and the Lagrangian velocity \mathbf{u}_{il}^L calculated from (5) could be very large and results in a numerical instability. If this velocity is used to calculate the strain rate in the cells around the node, an unphysical strain rate may be obtained and result in instability of the calculation. Therefore, for problems involving material interactions, the Lagrangian node velocity should

not be used to calculate the strain rate in a time explicit scheme. From (7) we find that such large node acceleration resulting from small mass on the node does not cause large acceleration of material points, because the large node velocity difference is multiplied by the same small value of the shape function, when the node velocity at time step $n+1$ is calculated from (9). The effects of the small mass on the node and the resulting instability have been greatly reduced. The strain rate should then be calculated using the node velocity obtained from (9) after the material points have been moved according to (8). With such calculated strain rate, the stress σ_{ip}^{n+1} can be updated using the constitutive relation of the material.

3.2 Calculation of volume fractions

Calculation of material interaction requires solving for volume fractions in the problem domain. The continuity condition requires that the volume fractions of all the materials sum to one. This condition is automatically satisfied in a single material case. For calculation of multi-material interactions, relation (4) is used to determine pressure in the system [3]. In MPM, the volume fractions are calculated as

$$\theta_i = \frac{1}{V_i} \sum_{p=1}^M v_{ip} S_i(\mathbf{x}_{ip}), \quad (10)$$

where v_{ip} is the volume of the material point p , and V_i is the control volume associated with node i . There is an error of $O[(\Delta x)^d]$ in this calculation of volume fraction, where $d=1$ if there is a sharp material interface and $d=2$ for a spatially smooth volume fraction. Therefore after summing such calculated volume fractions over all materials, equation (4) cannot be satisfied exactly and we can only have

$$\sum_{i=1}^M \theta_i = \sum_{i=1}^M \frac{\rho_i}{\rho_i^0(p_i)} = 1 + O[(\Delta x)^d]. \quad (11)$$

If we still force the right hand side of (11) to be one to find a pressure, the error will accumulate quickly. Only in a few time steps, the accumulated error will overwhelm the result and lead to failure of the calculation. To overcome this difficulty, one needs to find a way of satisfying the continuity condition (4) consistent with the working principle of the MPM method, namely, a weak solution to the governing equations. A weak form of (4) needs to be derived for the MPM method and is found [4] to be

$$\frac{\partial}{\partial t} \left(\sum_{i=1}^M \theta_i \right)_i + (\mathbf{u}_m)_i \cdot \nabla \left(\sum_{i=1}^M \theta_i \right)_i = 0, \quad (12)$$

where \mathbf{u}_m is the mixture velocity. Equation (12) can be physically interpreted as, that following mixture motion the volume fraction sum is “incompressible”.

4 NUMERICAL EXAMPLES

The numerical schemes outlined above have been implemented in our code named CartaBlanca [5]. Figure 1 shows a two-dimensional calculated spall of a porous solid. The porous solid is surrounded by air. The spall is caused by a plate impact on the top surface (shown as a dashed line in Fig. 1) of the bottom plate which has twice of thickness of the top

plate. The plates are made of the same material and are modeled as linear elastic until failure. The failure happens when the tensile stress exceeds a stress limit. Although in this calculation the effect of air is negligible, to demonstrate the capability of this combination of the averaged equation model and the advanced MPM, the air flow is explicitly calculated. In this calculation, the impact velocity is 100 m/s. The density of the material is 2700 kg/m³, Young's modulus is 70 GPa, and Poisson's ratio is set to zero. According to the analytical calculation of the elastic waves generated from the impact, the damage (shown in red) should occur at 1.12 μ s after impact. Our numerical results show damage at about 1.18 μ s.

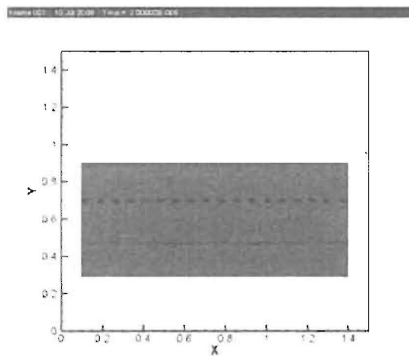


Figure 1. Snapshot of a spall calculation.

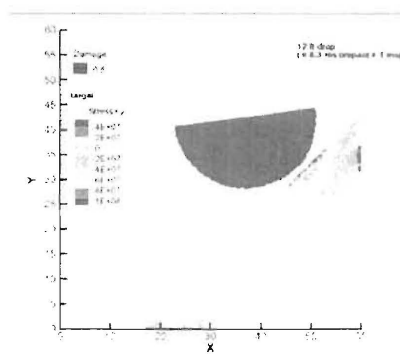


Figure 2. Calculated damage pattern (shown in red) and stress on the target.

As an application of the capability of modeling crack formation, we calculated the damage patterns in a half-cylinder dropped from 3.66 m. The result is shown in Fig. 2. Despite the 2-dimensional calculation performed, the result is in qualitative agreement with experimental results. A full 3-dimensional calculation is currently underway to compare with experiments in detail.

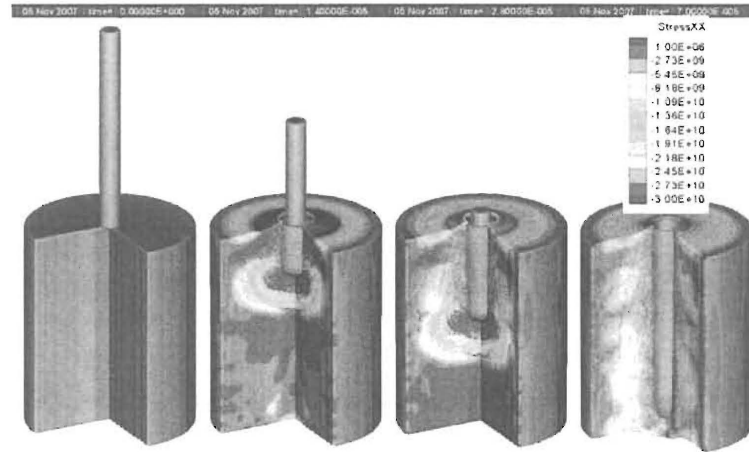


Figure 3. Snapshots of projectile-target interaction.

Figure 3 shows an axisymmetric calculation of penetration of a projectile into a cylinder of armor steel, where ductile properties of the material and the effects of large deformation are important. In this calculation the Johnson-Cook constitutive model [6] is used. This calculation indicates that as the projectile penetrates the target, the projectile material coats on the wall of the hole created by the projectile. Figure 4 shows the nose and tail positions of the projectile compared with experiments.

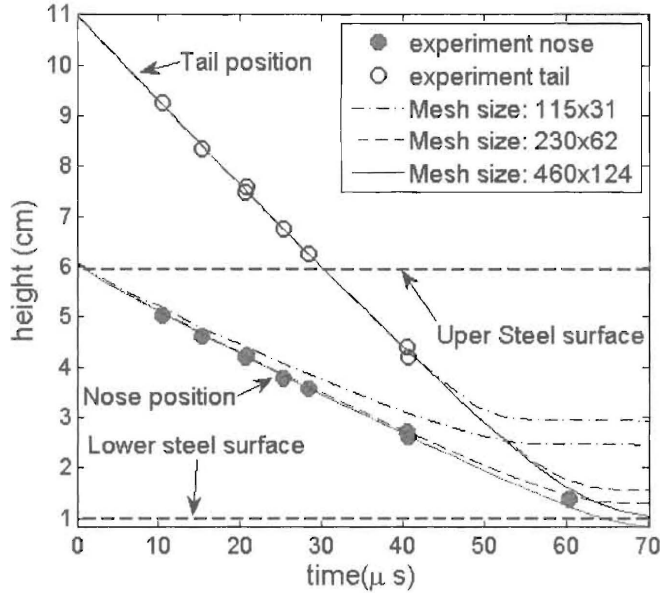


Figure 4. Comparison of nose and tail positions with experiment.

5 CONCLUSIONS

The combination of recent advances in the material point method and the continuous multiphase flow model, especially the multi-pressure model, has been shown to significantly enhance capability in numerically simulating multi-material interactions, especially for large deformations. Examples calculated using the multi-material interaction model and the enhanced MPM method show satisfactory comparison with theoretical and experimental results.

6 ACKNOWLEDGEMENT

This work was performed under the auspices of the United States Department of Energy.

REFERENCES

- [1] D. Sulusky, S.-J. Zhou, H. L. Schreyer, Application of a particle-in-cell method to solid mechanics, *Comput. Phys. Commun.* **87**, 236 (1995).
- [2] D. Z. Zhang, W. B. VanderHeyden, Q. Zou, N. T. Padial-Collins, Pressure calculations in

disperse and continuous multiphase flows, *Int. J. Multiphase Flow* **33**, 86 (2007).

[3] A Prosperetti, G. Tryggvason, *Computational Methods for Multiphase Flow*, Chapter 10, Cambridge University Press (2006).

[4] D. Z. Zhang, Q. Zou, . B. VanderHeyden, X. Ma, Material point method applied to multiphase flows. *J. Comput. Phys.* **227**, 3159 (2008).

[5] <http://www.lanl.gov/projects/CartaBlanca/>

[6] G. R. Johnson, W. H. Cook, Fracture characteristic of three metals subjected to various strains, strain rates, temperature and pressure, *Eng. Fract. Mech.* **21**, 31 (1985).